American Mineralogist, Volume 78, pages 733–745, 1993

Li: An important component in igneous alkali amphiboles

Frank C. Hawthorne,* Luciano Ungaretti, Roberta Oberti, Piero Bottazzi
CNR Centro di Studio per la Cristallochimica e la Cristallografia, via Bassi 4, I-27100 Pavia, Italy
Gerald K. Czamanske
U.S. Geological Survey, 345 Middlefield Road, Menlo Park, California 94025, U.S.A.

Abstract

The crystal structures of 13 alkali amphiboles have been refined to R values of 1–2% using single-crystal Mo$K\alpha$ X-ray data. Crystals used in the collection of the intensity data were subsequently analyzed by electron and ion microprobe. Site occupancies were assigned by site-scattering refinement and stereochemical considerations, taking into account the electron and ion microprobe analysis of each crystal. These alkali amphiboles are primarily eckermannite-arfvedsonite from peralkaline granites. Their X-ray scattering behavior is very different from most other monoclinic amphiboles; they show anomalously low scattering at the M3 site relative to that observed at the M1 and M2 sites. Ion microprobe analysis confirmed the presence of significant amounts of Li, up to 0.61 apfu (~1.0 wt% Li_2O), that the scattering results show to be completely ordered at the M3 site. These amphiboles contain significant amounts of Mn, up to 0.92 apfu (~6.9 wt% MnO), and minor Zn; the Mn is dominantly divalent and is distributed over the M1, M2, and M3 sites. Fe^{3+}/Fe^{2+} ratios were assigned on the basis of mean bond length considerations.

Li enters the arfvedsonite structure primarily by means of the substitution $^{[M3]}Li + Fe^{3+} \rightarrow {}^{[M3]}Fe^{2+} + Fe^{2+}[LiFe^{3+}(Fe^{2+})_{-2}]$ giving rise to the ideal end-member $NaNa_2Fe^{2+}_2LiFe^{3+}_2Si_8O_{22}(OH)_2$. The dominant compositional variation among the alkali amphiboles examined here is from manganoan arfvedsonite toward this Li-bearing end-member; an additional minor nyboitic substitution occurs but decreases with increasing Li content. Examination of the analytical data for these amphiboles, together with various formula renormalization procedures, shows that apparent anomalies in alkali amphibole stoichiometry (Si contents > 8 apfu; low C-group cation sums; A-site sums exceeding 1 apfu) are due to incomplete chemical analyses (specifically, no determination of Li and H_2O) and incorrect assumptions in the renormalization procedures (e.g., OH + F = 2.0 apfu). In addition, the anomalously high Fe^{3+}/Fe^{2+} ratios reported in previous wet-chemical studies are probably the result of (unrecognized) incorporation of Li into the structure by the substitution proposed above. By using the standard compositional criteria, the identification of only two distinct compositional trends in alkali amphiboles from silica-saturated peralkaline igneous rocks (magmatic-subsolidus and oxidizing, with the inference that the magmatic-subsolidus trend must be reducing) is invalid. The amphiboles examined here are classified as magmatic subsolidus by the usual criteria but have as high or higher ratios of $Fe^{3+}/(Fe^{2+} + Fe^{3+})$ than the riebeckitic compositions designated as oxidized, the high Fe^{3+} contents occurring in the structure in concert with increasing Li content. It is essential that Fe^{3+}/Fe^{2+} ratios be measured if amphibole compositions are to be used to derive information on redox conditions of crystallization.

Introduction

Alkali amphiboles are common constituents of silica-oversaturated peralkaline granitic rocks, and there have been many studies of their chemical evolution with progressive crystallization (Borley, 1963; de Keyser, 1966; Fabriès and Rocci, 1972; Neumann, 1976). A general consensus has emerged that amphibole compositional trends are strongly related to host-rock chemistry in alkaline rocks. Most important is the silica activity of the magma, as examined in detail by Giret et al. (1980); in silica-undersaturated rocks, the amphiboles are silica-poor (Si < 7.0 apfu), whereas in silica-oversaturated rocks, the amphiboles are silica-rich (6.8 < Si < 8.0 apfu). However, even within the silica-oversaturated rocks, further complexities are apparent. Comparing the behavior of alkali amphiboles with that of biotite, Czamanske and Wones (1973) recognized that, in the magmatic environment, progressive reducing and oxidizing processes pro-

* Present address: Department of Geological Sciences, University of Manitoba, Winnipeg, Manitoba R3T 2N2, Canada.

0003–004X/93/0708–0733$02.00

TABLE 1. Details of sample numbering and provenance for Li-bearing alkali amphiboles

No.	IMA name	Sample	Seq*	Provenance
A(1)	Magnesio-ferri-fluor-oxy-katophorite	82L42A-4	489	Amalia Tuff
A(2)	Magnesio-ferri-fluor-katophorite	82L42A-2	487	Amalia Tuff
A(3)	Ferro-fluor-leakeite	82QC49/4-2	456	Canada Pinabete pluton
A(4)	Ferro-fluor-leakeite	82QC49/100-2	428	Canada Pinabete pluton
A(5)	Ferro-fluor-leakeite	82QC49/1-2	454	Canada Pinabete pluton
A(6)	Mangesio-ferri-fluor-katophorite	83QC30-5	442	Virgin Canyon pluton
A(7)	Mangesio-ferri-fluor-katophorite	Q83J63-1	443	Virgin Canyon pluton
A(8)	Fluor-arfvedsonite	Q83J70-3	458	Virgin Canyon pluton
A(9)	Fluor-arfvedsonite	Q83J71-3	459	Virgin Canyon pluton
A(10)	Fluor-arfvedsonite	Q83J124-3	483	peralkaline rhyolite
A(11)	Fluor-arfvedsonite	Q83J124-1	482	peralkaline rhyolite
A(12)	Arfvedsonite	84QC7-1	440	Canada Pinabete pluton
A(13)	Arfvedsonite	PV9745	134	Pavia Mineral Museum

* Sequence number in amphibole refinement data bank at Pavia.

duce different chemical trends in amphibole compositions in granitic rocks. This aspect of amphibole behavior was examined in more detail by Strong and Taylor (1984); they identified two distinct trends of amphibole composition in these rocks, a magmatic-subsolidus trend (barroisite → richterite → arfvedsonite) of the form $SiNa \rightarrow {}^{[4]}AlCa$ and an oxidation trend of the form $^{[4]}AlFe^{3+} \rightarrow SiFe^{2+}$ or $^{A}\square Fe^{3+} \rightarrow {}^{A}NaFe^{2+}$ that terminates at riebeckite. These relations are of considerable potential use in evaluating the relative importance of primary magmatic and secondary hydrothermal processes in the emplacement and solidification of silica-oversaturated peralkaline granites.

Czamanske and Dillet (1988) examined chemical variations in a series of alkali amphiboles from peralkaline granites at Questa, New Mexico. They reviewed the published analytical data on arfvedsonitic amphiboles and emphasized the unsatisfactory nature of many alkali amphibole analyses. This point was also considered by Hawthorne (1976), who concluded either that Li is a significant octahedral site component in many of these amphiboles or that Na (or Ca?) may occur at the M1, M2, and M3 sites. Czamanske and Dillet (1988) further emphasized that the apparent trends of evolving amphibole composition in peralkaline granites cannot be considered reliable or even established because of the unsatisfactory nature of the amphibole formulae as indicated by the criteria of Leake (1968). In order to resolve these compositional problems with the alkali amphiboles, we have examined a well-documented series of alkali amphiboles by crystal-structure refinement and electron and ion microprobe analyses.

EXPERIMENTAL METHODS

Sample descriptions and petrologic setting

The sample codes and names (IMA-approved nomenclature) of the amphibole crystals used in this work are indicated in Table 1, sorted in order of increasing cell volume. Crystals A(1–12) are from the Questa caldera, New Mexico, and details of their occurrence and paragenesis are given by Czamanske and Dillet (1988). The broader petrogenetic context in which these amphiboles occur was discussed by Johnson et al. (1989, 1990). At Questa, alkali amphibole has been found in mildly peralkaline rocks making up the Amalia Tuff (>500 km³ in erupted volume), overlying rhyolitic lava, a ring dike, and marginal facies of two small plutons intrusive into the caldera floor. Commonly, alkali amphibole occurs in association with tetrasilicic mica and sodic pyroxene in rocks that contain 75–77 wt% SiO_2. Petrogenetic, geochemical, and stratigraphic evidence suggest that the peralkaline rhyolite was a last erupted pulse of the Amalia Tuff and that the peralkaline intrusive rocks (which seem to form screens against metaluminous granite that are 30 m thick) represent unerupted parts of the tuff-forming magma. Czamanske and Dillet (1988, their Table 5) document strong zoning of alkali amphibole grains as large as 0.2

TABLE 2. Miscellaneous data collection and structure refinement information for Li-bearing alkali amphiboles

	A(1)	A(2)	A(3)	A(4)	A(5)	A(6)	A(7)	A(8)	A(9)	A(10)	A(11)	A(12)	A(13)
a (Å)	9.795	9.808	9.792	9.796	9.792	9.835	9.861	9.816	9.815	9.858	9.859	9.840	9.986
b (Å)	17.993	17.993	17.934	17.934	17.935	17.944	18.050	18.004	18.016	18.046	18.049	18.036	18.042
c (Å)	5.280	5.284	5.313	5.312	5.314	5.297	5.288	5.325	5.329	5.316	5.316	5.365	5.314
β (°)	104.53	104.54	103.87	103.89	103.85	103.97	104.22	103.72	103.71	103.69	103.69	104.05	103.92
V (Å³)	900.88	902.58	905.81	906.07	906.11	907.11	912.39	914.26	915.52	918.84	919.08	923.67	929.33
θ_{max} (°)	30	30	30	40	30	30	30	35	30	30	35	30	40
D_c	3.19	3.18	3.34	3.33	3.35	3.29	3.24	3.39	3.38	3.35	3.37	3.38	3.42
F_o	1371	1369	1376	1986	1377	1384	1382	2084	1389	1391	2097	1392	2121
$F_o > 5\sigma$	755	880	1067	1719	1078	942	1120	1376	974	1129	1663	947	1923
R_{sym}	2.4	2.9	1.5	3.7	1.6	2.7	1.8	1.6	1.8	1.3	1.2	2.8	1.3
R_{obs}	1.8	1.7	1.3	1.9	1.3	1.6	1.4	1.5	1.7	1.3	1.4	1.6	1.3
R_{all}	5.3	3.8	2.3	2.3	2.3	3.0	2.4	3.3	3.1	2.0	2.2	3.2	1.7

TABLE 4. Selected interatomic distances (Å) in Li-bearing alkali amphiboles

	A(1)	A(2)	A(3)	A(4)	A(5)	A(6)	A(7)	A(8)	A(9)	A(10)	A(11)	A(12)	A(13)
T1-O1	1.621	1.617	1.609	1.610	1.608	1.610	1.615	1.613	1.615	1.610	1.610	1.615	1.602
-O5	1.636	1.635	1.630	1.631	1.631	1.627	1.633	1.631	1.630	1.630	1.631	1.641	1.629
-O6	1.635	1.637	1.629	1.629	1.630	1.634	1.631	1.630	1.628	1.626	1.625	1.636	1.627
-O7	1.624	1.624	1.631	1.631	1.631	1.627	1.637	1.629	1.629	1.634	1.635	1.632	1.636
⟨T1-O⟩	1.629	1.628	1.625	1.626	1.625	1.625	1.629	1.626	1.626	1.625	1.625	1.631	1.624
T2-O2	1.625	1.624	1.621	1.622	1.621	1.615	1.618	1.624	1.624	1.621	1.621	1.621	1.615
-O4	1.591	1.593	1.596	1.597	1.595	1.583	1.590	1.595	1.598	1.594	1.596	1.594	1.586
-O5	1.642	1.645	1.653	1.652	1.652	1.653	1.651	1.651	1.650	1.655	1.654	1.656	1.665
-O6	1.660	1.658	1.659	1.659	1.658	1.658	1.666	1.657	1.659	1.668	1.667	1.669	1.669
⟨T2-O⟩	1.630	1.630	1.632	1.633	1.631	1.627	1.631	1.632	1.633	1.635	1.634	1.635	1.634
M1-O1 × 2	2.061	2.062	2.092	2.089	2.092	2.074	2.074	2.105	2.105	2.102	2.104	2.117	2.108
-O2 × 2	2.093	2.092	2.111	2.107	2.115	2.067	2.065	2.102	2.108	2.080	2.082	2.100	2.106
-O3 × 2	1.996	2.004	2.094	2.091	2.097	2.084	2.087	2.124	2.127	2.124	2.125	2.128	2.123
⟨M1-O⟩	2.050	2.053	2.099	2.096	2.101	2.075	2.075	2.110	2.113	2.102	2.104	2.115	2.112
M2-O1 × 2	2.173	2.167	2.113	2.115	2.113	2.174	2.188	2.142	2.139	2.187	2.184	2.152	2.152
-O2 × 2	2.079	2.076	2.037	2.039	2.036	2.075	2.084	2.044	2.041	2.071	2.070	2.068	2.076
-O4 × 2	1.976	1.973	1.931	1.932	1.931	1.972	1.985	1.932	1.929	1.960	1.956	1.938	1.953
⟨M2-O⟩	2.076	2.072	2.027	2.029	2.026	2.073	2.086	2.039	2.036	2.073	2.070	2.053	2.061
M3-O1 × 4	2.075	2.083	2.114	2.113	2.116	2.085	2.080	2.120	2.126	2.104	2.106	2.122	2.135
-O3 × 2	2.023	2.038	2.115	2.113	2.113	2.063	2.052	2.103	2.106	2.088	2.091	2.119	2.093
⟨M3-O⟩	2.057	2.068	2.114	2.113	2.115	2.077	2.071	2.115	2.119	2.098	2.101	2.121	2.121
M4-O2 × 2	2.423	2.435	2.423	2.422	2.421	2.408	2.416	2.426	2.435	2.421	2.419	2.419	2.421
-O4 × 2	2.348	2.359	2.357	2.358	2.355	2.336	2.338	2.352	2.352	2.341	2.340	2.363	2.370
-O5 × 2	2.792	2.794	2.884	2.887	2.888	2.873	2.862	2.909	2.905	2.938	2.941	2.930	2.945
-O6 × 2	2.514	2.515	2.503	2.503	2.503	2.548	2.564	2.511	2.508	2.549	2.550	2.531	2.582
⟨M4-O⟩ × 2	2.519	2.526	2.542	2.542	2.542	2.541	2.545	2.550	2.550	2.562	2.563	2.561	2.580
$^{[12]}$⟨A-O⟩	2.928	2.925	2.919	2.918	2.920	2.915	2.920	2.934	2.939	2.919	2.921	2.943	2.951
⟨Am-O⟩	2.841	2.841	2.828	2.828	2.828	2.835	2.843	2.836	2.841	2.830	2.830	2.842	2.866
⟨A2-O⟩	2.710	2.682	2.616	2.595	2.644	2.676	2.683	2.583	2.526	2.600	2.613	2.596	2.663

× 2.0 mm. Early-formed amphibole is enriched in Mg and Ca, and late amphibole is enriched in Fe and Na; alkali amphibole compositions range from katophorite to arfvedsonite. The crystals examined here were selected from samples in which amphibole zoning was minimal but the amphibole compositions span the entire observed range.

X-ray data collection and structure refinement

Experimental details are as described by Oberti et al. (1992). Unit-cell, *R*-value, and other data are in Table 2. Final atomic coordinates and equivalent isotropic displacement parameters are given in Table 3,[1] selected interatomic distances are given in Table 4, and the refined site-scattering powers are listed in Table 5. Anisotropic displacement parameters and observed and calculated structure factors may be obtained from Pavia on request.

Microprobe analysis

Subsequent to the experimental crystallographic work, the crystals used in the collection of the intensity data were mounted, polished, and analyzed by electron and ion microprobe techniques, following the procedures described by Oberti et al. (1992) and Ottolini et al. (1992).

Calculation of the formula unit

Oberti et al. (1992) showed that $^{[6]}$Ti enters the richterite structure by means of the substitution $^{[M1]}Ti + 2^{[O3]}O^{2-} \rightarrow {}^{[M1]}(Mg,Fe) + 2^{[O3]}(OH)^{-}$. When this substitution occurs, assumption of two monovalent anions occupying the O3 site is not valid, and renormalization of the formula unit on the basis of 23 O atoms will give low C-group sums. In this case, the formula unit should be calculated

[1] A copy of Table 3 may be ordered as Document AM-93-529 from the Business Office, Mineralogical Society of America, 1130 Seventeenth Street NW, Suite 330, Washington, DC 20036, U.S.A. Please remit $5.00 in advance for the microfiche.

TABLE 5. Refined site-scattering values in Li-bearing alkali amphiboles

Site	A(1)	A(2)	A(3)	A(4)	A(5)	A(6)	A(7)	A(8)	A(9)	A(10)	A(11)	A(12)	A(13)
M1 × 2	16.9	15.6	22.3	21.7	22.8	16.8	15.7	24.4	24.5	22.1	22.7	24.2	25.7
M2 × 2	17.5	19.8	26.0	26.0	26.0	24.0	23.1	25.9	26.1	25.7	25.8	26.0	25.6
M3	13.8	12.9	10.4	10.5	10.6	14.5	14.0	17.6	18.0	16.5	17.2	20.6	20.8
M4 × 2	16.6	15.3	11.0	11.2	11.0	14.2	14.5	11.0	10.9	11.2	11.5	11.7	11.2
M4′ × 2	—	—	—	—	—	—	0.3	—	—	0.7	0.5	—	—
A	3.1	3.2	3.2	3.2	3.0	3.5	3.5	3.8	4.1	3.0	3.0	3.8	9.4
Am × 2	1.3	1.8	4.1	4.0	4.0	2.8	2.8	3.0	2.6	4.4	4.3	3.2	2.8
A2 × 2	0.5	0.5	0.2	0.2	0.3	0.9	0.7	0.1	—	0.3	0.3	0.1	0.6
O3 × 2	8.7	8.7	8.9	8.8	8.9	8.7	8.8	8.6	8.7	8.9	8.8	8.5	8.1

Note: Values are in electrons; estimated standard deviations are <0.1 e.

TABLE 6. Chemical analyses of crystals used in the structure refinement

	A(2)	A(5)	A(6)	A(7)	A(8)	A(9)	A(10)	A(11)	A(12)	A(13)
SiO_2	51.91	51.12	51.86	51.26	49.03	49.46	49.58	49.67	48.56	49.31
Al_2O_3	1.86	1.13	1.50	1.96	0.87	0.97	0.75	0.76	1.41	0.73
TiO_2	0.41	0.68	0.38	0.40	0.73	0.66	0.98	0.98	0.67	0.49
Fe_2O_3	6.77	16.73	13.98	6.79	14.51	14.12	10.17	10.56	12.58	11.13
FeO	6.45	8.87	5.11	8.64	13.70	14.40	15.47	14.32	18.43	24.43
MgO	13.36	2.02	8.85	11.50	0.61	0.87	2.75	3.23	1.23	0.02
MnO	3.82	4.51	4.35	4.30	5.46	5.30	6.66	6.92	3.38	1.09
ZnO	0.00	0.57	0.14	0.37	0.90	0.84	0.02	0.03	0.28	0.14
CaO	6.64	0.15	3.07	4.75	0.05	0.06	0.34	0.39	0.45	0.38
Na_2O	4.60	9.22	7.13	6.67	8.95	9.02	8.38	8.44	8.26	7.43
K_2O	0.82	1.19	1.10	0.92	1.29	1.37	1.01	0.91	1.15	2.90
Li_2O	0.11	0.99	0.27	0.09	0.60	0.54	0.38	0.39	0.21	0.29
F	2.91	2.87	2.43	2.89	2.85	2.66	3.15	3.28	1.90	0.37
H_2O	(0.65)	(0.55)	(0.85)	(0.65)	(0.52)	(0.63)	(0.39)	(0.33)	(1.00)	(1.68)
O = F	−1.23	−1.21	−1.02	−1.22	−1.20	−1.12	−1.33	−1.38	−0.80	−0.16
Total	99.08	98.82	100.36	99.60	97.97	98.94	98.68	98.80	98.43	100.09
					Chemical formulae					
Si	7.657	7.831	7.652	7.628	7.780	7.777	7.848	7.825	7.741	7.855
Al	0.323	0.169	0.261	0.344	0.163	0.180	0.140	0.141	0.259	0.137
Sum T	7.980	8.000	7.913	7.972	7.943	7.957	7.988	7.966	8.000	7.992
Al	0.000	0.035	0.000	0.000	0.000	0.000	0.000	0.000	0.006	0.000
Ti	0.045	0.078	0.042	0.045	0.087	0.078	0.117	0.116	0.080	0.059
Fe^{3+}	0.751	1.931	1.552	0.760	1.733	1.671	1.211	1.252	1.509	1.334
Fe^{2+}	0.796	1.137	0.631	1.075	1.818	1.894	2.048	1.887	2.457	3.255
Mg	2.938	0.461	2.057	2.551	0.144	0.204	0.649	0.759	0.292	0.005
Mn	0.477	0.585	0.544	0.542	0.734	0.706	0.893	0.923	0.456	0.147
Zn	0.000	0.064	0.015	0.041	0.105	0.098	0.002	0.003	0.033	0.016
Li	0.065	0.610	0.160	0.054	0.383	0.341	0.242	0.247	0.135	0.186
Sum C	5.072	4.901	5.001	5.068	5.004	4.992	5.162	5.187	4.968	5.002
C − 5	0.072	0.000	0.001	0.068	0.004	0.000	0.162	0.187	0.000	0.002
Ca	1.049	0.025	0.485	0.757	0.009	0.010	0.058	0.066	0.077	0.065
Na	0.879	1.975	1.514	1.175	1.987	1.990	1.780	1.747	1.923	1.933
Sum B	2.000	2.000	2.000	2.000	2.000	2.000	2.000	2.000	2.000	2.000
Na	0.437	0.763	0.526	0.749	0.767	0.760	0.792	0.833	0.630	0.362
K	0.154	0.233	0.207	0.175	0.261	0.276	0.204	0.183	0.234	0.589
Sum A	0.591	0.996	0.733	0.924	1.028	1.036	0.996	1.016	0.864	0.951
F	1.352	1.408	1.143	1.360	1.448	1.338	1.559	1.616	0.963	0.187
OH	0.648	0.592	0.857	0.640	0.552	0.662	0.441	0.384	1.037	1.813

on the basis of (23 + $^{[6]}$Ti) O atoms (allowing of course for analyzed F content). Here, we decided on the presence or absence of this particular substitution by examining the lengths of the M1-O and M3-O bonds to O3 relative to O1 and O2. Fe^{3+}/Fe^{2+} ratios were calculated from the structural results and put back into the normalization process; this calculation was repeated until all values were self-consistent, and the Fe^{3+}/Fe^{2+} ratios assigned (Table 6) reflected the final structural results.

Discussion

The general features of the arfvedsonite structure were characterized by Kawahara (1963) and Hawthorne (1978), and the current results are broadly compatible with previous findings. However, there are some significant differences that distinguish the general chemical composition and site populations of the amphiboles examined in this work. In particular, crystals A(1–13) were selected on the basis of their scattering at the M3 site, which is anomalously lower than that observed at the M1 and M2 sites in the same crystal. Analysis of Li content by ICP for two bulk alkali-amphibole separates from Questa gave 1320 and 1400 ppm Li, respectively. These two features suggest that Li is playing an important role in these alkali amphiboles.

The tetrahedral sites

Stereochemical details of the $^{[4]}$T1 and $^{[4]}$T2 sites are given in Table 4. The T-group occupancies assigned from the microprobe analyses are given in Table 6; Si + Al_{tot} ~ 8.0 apfu, and the grand mean value of this sum is 7.975 ± 0.034. The fact that this value is statistically equal to the total number of T sites in the formula unit, combined with the fact that the variation in ⟨T1-O⟩ with Al_{tot} (Fig. 1) agrees with the analogous curve of Hawthorne and Grundy (1977), suggests that all Al is tetrahedrally coordinated in these amphiboles.

The octahedral sites: Scattering considerations

There are three sites with octahedral coordination, M1, M2, and M3. Because there are more than two scattering species per site, the total site scattering cannot give a unique solution for the site populations (Hawthorne, 1983b). For most chemically simple amphiboles, however, the microprobe analyses and the detailed stereochemical variations that accompany the changes in site chemistry can be used in conjunction with the scattering results to give reliable site populations (Ungaretti et al., 1983). The microprobe analyses (Table 6) indicate significant amounts of Fe, Mn, Mg, Al, Li, Zn, and Ti at the

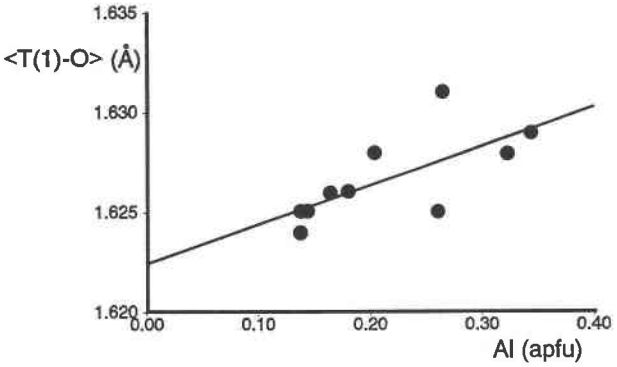

Fig. 1. Variation in ⟨T1-O⟩ as a function of Al content of the amphibole.

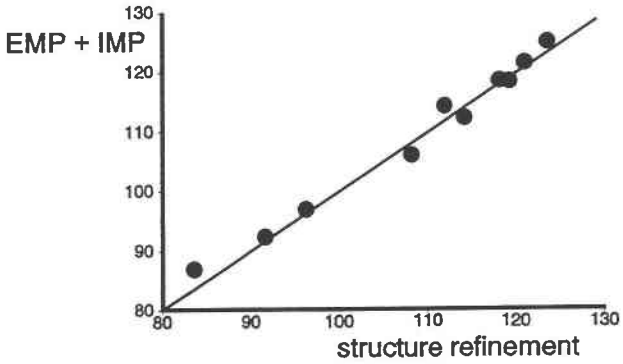

Fig. 2. Comparison of the total refined scattering (in electrons) at the M1, M2, and M3 sites with the analogous values calculated from the C-group cations of the formula unit derived from the electron (EMP) and ion (IMP) microprobe analyses.

octahedral sites; in addition, Fe and Mn can occur both in divalent and trivalent states. For scattering purposes, it is often convenient to group species of similar scattering power together; thus $Fe' = (Fe^{2+} + Fe^{3+} + Mn^{2+} + Mn^{3+} + Zn)$ and $Mg' = (Mg + Al)$.

The behavior of Ti. In the past, $^{[6]}Ti$ was assigned to the M2 site (except in oxy-kaersutite, Kitamura et al., 1975). This assignment was purely speculative, based on the fact that $^{[6]}Ti$ is a small highly charged cation and seemed likely to behave like other small highly charged C-group cations (i.e., Fe^{3+} and Al) in amphiboles. Oberti et al. (1992) have shown that in richterite, $^{[6]}Ti$ is ordered at M1, not M2. In the amphiboles examined here, $^{[6]}Ti^{4+}$ could order at M1 or M2, which is the case in each of the crystals examined, as evaluated from the local stereochemistry around the M1 site.

Total scattering at M1, M2, and M3. The site-scattering values were unconstrained in the refinement procedure, and the total scattering at the M1, M2, and M3 sites represents the total number of electrons (the mean atomic number when expressed per position) for the cations at these positions. These values can also be derived from the unit formulae calculated from the microprobe analyses, and comparison of these values gives a check on the consistency of both sets of results. A graphical comparison is given in Figure 2. The results closely follow the 1:1 line ($R = 0.999$), indicating that there is no systematic difference between the two sets of results and suggesting that there is no significant systematic error in either of the two sets of results. The root-mean-square deviation is 1.74 electrons (e), corresponding to ~0.35 e per site [~0.02 atoms for occupancy by (Mg,Fe)].

Scattering at M1 and M3. The refined scattering values at the M1 and M3 sites are shown in Figure 3. Also shown is the range of values found for ~550 monoclinic amphiboles. Most samples show increased scattering at M1 correlating with increased scattering at M3, and the data define a well-bounded lunette; for amphiboles with Mg and Fe^{2+} at these sites, this can be described as the compositional (ordering) space bounded by $0.4 < K_d < 1.0$, where K_d is the distribution coefficient (Ungaretti et al., 1978). For the amphiboles of this study (together with a few other alkali amphiboles all containing $^{[6]}Li$; Ungaretti et al., 1978; Hawthorne, 1978; Ghose et al., 1986), the site-scattering values are very different. They fall outside the well-defined field of all other refined amphiboles, and the scattering at M1 is always greater than the scattering at M3, opposite to that observed in nearly all other amphiboles (Fig. 3).

Ion microprobe analyses (this study) and wet-chemical analyses (Czamanske and Dillet, 1988) of some of these amphiboles have significant Li contents. The X-ray scattering powers of the elements are proportional to their atomic numbers. Li ($Z = 3$) scatters much less strongly than Mg ($Z = 12$) and Fe ($Z = 26$), the other important

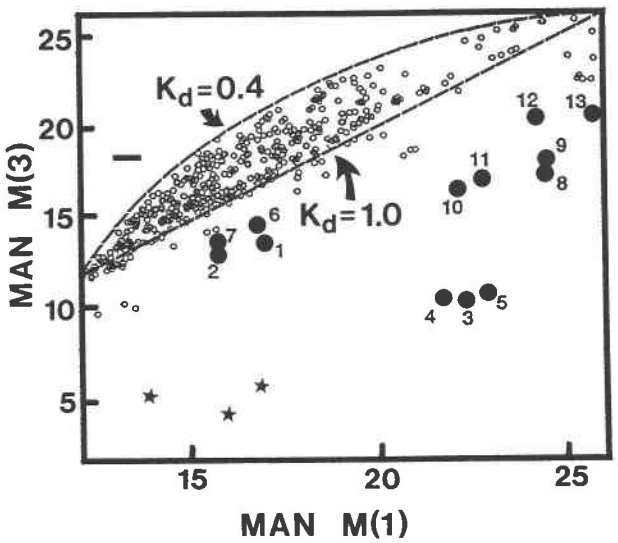

Fig. 3. Refined total scattering powers at M1 and M3 in the alkali amphiboles of this study (numbered solid circles) compared with the distribution of values observed for ~550 refined monoclinic amphiboles (open circles) and three leakeite samples (stars). The refined scattering at each site is expressed as the m.a.n. (mean atomic number) of the atoms at the site; thus m.a.n. values of 12 and 26 correspond to Mg and Fe, respectively.

TABLE 7. Octahedral site populations obtained from the results of the structure refinement and from EMP and IMP estimates for minor elements

	M1							M2								
	Mg	Fe^{2+}	Fe^{3+}	Ti	Mn	d_{obs}	d_{calc}	Mg	Fe^{2+}	Fe^{3+}	Ti	Mn	Zn	Al	d_{obs}	d_{calc}
A(1)	0.640	—	0.265	0.025	0.070	2.050	2.050	0.595	—	0.275	—	0.130	—	—	2.076	2.075
A(2)	0.730	—	0.200	0.025	0.045	2.053	2.053	0.435	—	0.400	—	—	0.165	—	2.072	2.072
A(3)	0.250	0.560	—	—	0.190	2.099	2.099	—	0.020	0.910	0.040	—	0.030	—	2.027	2.027
A(4)	0.300	0.530	—	—	0.170	2.096	2.096	—	0.030	0.900	0.035	—	0.035	—	2.029	2.029
A(5)	0.210	0.590	—	—	0.200	2.101	2.101	—	—	0.930	0.035	—	0.035	—	2.026	2.026
A(6)	0.635	—	0.110	0.020	0.235	2.075	2.075	0.140	0.425	0.425	—	—	0.010	—	2.073	2.073
A(7)	0.715	—	0.035	0.020	0.230	2.075	2.075	0.210	0.440	0.290	—	0.040	0.020	—	2.086	2.085
A(8)	0.100	0.680	—	—	0.220	2.110	2.110	—	0.130	0.770	0.050	—	0.050	—	2.039	2.039
A(9)	0.090	0.640	—	—	0.270	2.113	2.113	—	0.100	0.810	0.040	—	0.050	—	2.036	2.037
A(10)	0.260	0.450	—	—	0.290	2.102	2.102	—	0.470	0.470	0.060	—	—	—	2.073	2.072
A(11)	0.210	0.500	—	—	0.290	2.104	2.104	—	0.500	0.440	0.060	—	—	—	2.070	2.070
A(12)	0.110	0.720	—	—	0.170	2.115	2.114	—	0.290	0.650	0.040	—	0.020	—	2.053	2.052
A(13)	0.020	0.980	—	—	—	2.112	2.115	—	0.340	0.600	0.030	—	0.010	0.020	2.061	2.061

C-group species in amphiboles; hence the occurrence and strong ordering of Li over the octahedrally coordinated sites in the amphibole structure greatly perturbs the usual site-scattering relations for amphiboles, and Figure 3 suggests that Li in these amphiboles is strongly ordered at the M3 site. Note that this is in accord with direct site-occupancy refinements for three riebeckite samples (Hawthorne, 1978; Ungaretti et al., 1978) in which only Fe (+ Mn) and Li occur at the C-group sites.

Figure 4 shows the scattering at M3, with lines delineating the substitutions Li → Fe′ and Li → Mg at this site. For low Mg contents, the data fall on or close to the Li → Fe′ line, confirming that the scattering is dominated by Fe′ and Li. As the Mg content increases, the points fall further away from the Li → Fe′ line, indicating a more equal partitioning of Mg over M1 and M3 at higher Mg contents.

Scattering at M2. The refined site-scattering values

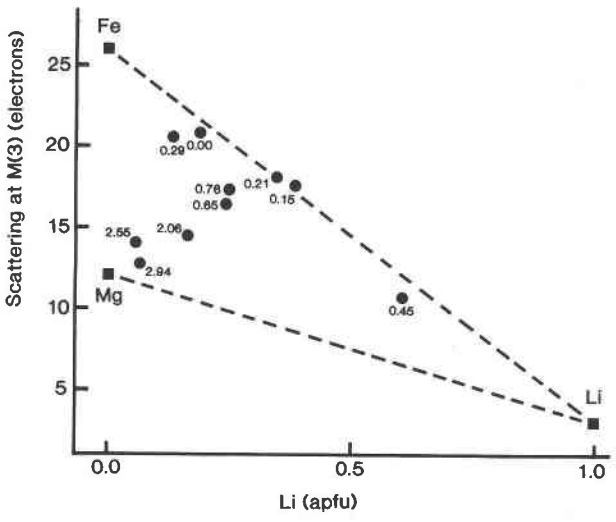

Fig. 4. Variation in scattering at M3 as a function of Li content of the formula unit for the alkali amphibole structures refined in the current study; the numbers by the symbols indicate the Mg content in apfu.

Table 5) show this site to be dominated by Fe′, except in the most Mg-rich crystals. Possible light atom constituents of this site are Al and Mg, as all Li occupies M3. For crystals A(3–5, 8–13), the mean M2 site scattering is 25.92 e, indicating negligible Mg and Al at the M2 site in these crystals. For the remaining crystals, A(1, 2, 6, 7), the site scattering may be expressed as Mg and Fe.

The octahedral sites: Stereochemical considerations

A complete chemical interpretation of the m.a.n. (mean atomic number) values obtained from the site-scattering refinements requires that the mean bond lengths obtained from the structure refinement be taken into account. Inspection of Table 4 indicates that there are at least two distinct crystal-chemical situations. In one case [crystals A(1), A(2), A(6), and A(7)], ⟨M1-O⟩ and ⟨M3-O⟩ are short (Table 4), indicating the presence of smaller tri- and tetravalent cations at M1 and M3. Following Oberti et al. (1992), Ti was assigned to M1 in these crystals, and the remaining transition metals at M1 and M3 were assigned as Fe^{3+}; the observed mean bond lengths (Table 7) confirm this assignment. For the remaining crystals, the ⟨M1-O⟩ and ⟨M3-O⟩ distances are compatible with divalent transition metals at M1 and M3.

A further factor to be taken into account when determining site populations is the presence of F at the O3 site, as that significantly affects ⟨M1-O⟩ and ⟨M3-O⟩ distances (Hawthorne, 1983a).

In order to derive complete octahedral site populations in amphiboles, it is necessary to take into account the following crystal-chemical constraints: (1) complete occupancy of each site, (2) overall charge balance, (3) observed m.a.n., (4) observed ⟨M-O⟩ distances (Ungaretti et al., 1983). In this way, it is possible to obtain reliable site populations (*x, y, z, w*) for up to four cations (*A, B, C, D*) at each octahedral site in the amphibole structure by solving the following system of simultaneous equations:

$$x + y + z + w = 1.0 \quad (1)$$

$$xC_A + yC_B + zC_C + wC_D = C_{site} \quad (2)$$

TABLE 7.—*Continued*

M3						
Li	Mg	Fe^{2+}	Fe^{3+}	Mn	d_{obs}	d_{calc}
0.060	0.770	—	0.140	0.030	2.057	2.058
0.060	0.830	—	0.040	0.070	2.068	2.068
0.640	0.040	—	—	0.320	2.114	2.112
0.640	0.040	—	—	0.320	2.113	2.113
0.630	0.040	—	—	0.330	2.115	2.114
0.160	0.550	0.160	0.060	0.070	2.077	2.077
0.080	0.720	0.190	—	0.010	2.071	2.070
0.360	—	0.410	—	0.230	2.115	2.114
0.330	—	0.420	—	0.250	2.119	2.115
0.250	0.250	0.280	—	0.220	2.098	2.099
0.250	0.200	0.330	—	0.220	2.101	2.101
0.170	0.090	0.500	—	0.240	2.121	2.118
0.220	—	0.640	—	0.140	2.121	2.122

$$xZ_A + yZ_B + zZ_C + wZ_D = Z_{site} \quad (3)$$

$$x\langle M\text{-}O\rangle_A + y\langle M\text{-}O\rangle_B + z\langle M\text{-}O\rangle_C + w\langle M\text{-}O\rangle_D = \langle M\text{-}O\rangle_{site} \quad (4)$$

where C_I is the formal charge of the Ith cation and Z_I is the atomic number of the Ith cation. The contribution of any other (minor) components can be calculated from the electron and ion microprobe results and subtracted from the values on the right side of the equations before solving the system.

In the amphiboles examined here, Li, Mg, Ti, Mn^{2+}, Mn^{3+}, Fe^{2+}, Fe^{3+}, and Zn can be present at the octahedral sites ($^{[6]}Al$ is essentially absent in these crystals). In order to reduce the number of unknown parameters, we applied the following constraints, based on the crystal-chemical arguments expressed above: (1) Li orders at M3 and is deduced from the ion microprobe analysis; (2) Zn orders at M2 and is deduced from the electron microprobe analysis; (3) Ti orders at the M1 site when dehydroxylation is present [crystals A(1), A(2), A(6), and A(7)]; otherwise Ti orders at M2; Ti content is deduced from the electron microprobe analysis; (4) All Mn is in the divalent state; this is supported by the fact that a significant proportion of the Fe is still in the divalent state. The number of unknowns is reduced to four at each octahedral site, and it is now possible to determine the site populations from the above system of equations.

For the crystals refined here, the site populations at the A and M4 sites were obtained from the electron microprobe analyses (Table 6) and from the refined site-scattering values (Table 5). For the T1 site, the Al content was evaluated from the electron microprobe analyses and the observed ⟨T1-O⟩ values. In this way, the residual positive charge at the octahedral sites was obtained. The following end-member bond lengths were used for each cation: Li = 2.118, Mg = 2.078, Al = 1.925, Ti = 1.985, Mn^{2+} = 2.170, Fe^{2+} = 2.120, Fe^{3+} = 2.025, Zn = 2.098 Å, after correction in the case of the M1 and M3 sites for the F content from the electron microprobe analyses. For this purpose, a correction equal to −0.013 Å per F apfu (Oberti et al., 1993) was used in the calculation of ⟨M1-O⟩ and ⟨M3-O⟩. The resultant octahedral site populations and the corresponding observed and calculated mean bond lengths are given in Table 7, and the resultant chemical formulae are listed in Table 8.

Scattering at O3

It is usually not considered feasible to derive information on F → OH substitution directly from scattering results, as the atomic numbers of F and O differ only by one. However, we attempted it by unconstrained refinement of the scattering at the O3 site (Table 5). Comparison of the refined electrons at O3 (epfu) and the F content of the formula unit calculated from the microprobe analyses (Fig. 5) shows scatter about the 1:1 line. There is a tendency for the scattering to be slightly higher than that expected from the analyses, but it is fairly small in view of the fact that these amphiboles are generally quite Fe-rich and hence show high absorption of both scattered (diffraction) and fluorescent (electron microprobe) X-rays.

Scattering at M4

Comparison of the refined scattering at M4 with the B-group cations assigned from the microprobe analyses by the formula unit calculation is shown in Figure 6. By

TABLE 8. Complete chemical formulae obtained from the results of the structure refinement and from EMP and IMP estimates for minor elements

	A		M4				M1 + M2 + M3								T1 + T2			W	
	K	Na	Na	Ca	Mn	Fe	Li	Mg	Fe^{2+}	Fe^{3+}	Ti	Mn	Zn	Al	Si	Al	O^{2-}	OH	F
A(1)	0.15	0.36	1.75	0.25	—	—	0.06	3.24	—	1.22	0.05	0.43	—	—	7.58	0.42	22.60	—	1.40
A(2)	0.17	0.42	1.05	0.95	—	—	0.06	3.16	—	1.24	0.05	0.49	—	—	7.64	0.36	22.46	0.18	1.36
A(3)	0.24	0.67	2.00	—	—	—	0.64	0.54	1.16	1.82	0.08	0.70	0.06	—	7.75	0.25	22.00	0.30	1.70
A(4)	0.24	0.66	2.00	—	—	—	0.64	0.64	1.12	1.80	0.07	0.66	0.07	—	7.80	1.20	22.00	0.40	1.60
A(5)	0.24	0.66	2.00	—	—	—	0.63	0.46	1.18	1.86	0.07	0.73	0.07	—	7.73	0.27	22.00	0.40	1.60
A(6)	0.21	0.63	1.28	0.72	—	—	0.16	2.11	1.00	1.13	0.04	0.54	0.02	—	7.79	0.21	22.40	0.22	1.38
A(7)	0.17	0.68	1.20	0.72	0.08	—	0.08	2.57	1.07	0.65	0.04	0.55	0.04	—	7.70	0.30	22.00	0.40	1.60
A(8)	0.25	0.48	1.99	0.01	—	—	0.36	0.20	2.03	1.54	0.10	0.67	0.10	—	7.88	0.12	22.00	0.80	1.20
A(9)	0.26	0.41	2.00	—	—	—	0.33	0.18	1.90	1.62	0.08	0.79	0.10	—	7.88	0.12	22.00	0.60	1.40
A(10)	0.18	0.82	1.83	0.08	0.09	—	0.25	0.77	2.22	0.84	0.12	0.80	—	—	8.00	—	22.00	0.30	1.70
A(11)	0.16	0.84	1.83	0.06	0.11	—	0.25	0.62	2.33	0.88	0.12	0.80	—	—	7.96	0.04	22.00	0.30	1.70
A(12)	0.22	0.54	1.87	0.08	—	0.05	0.17	0.31	2.52	1.30	0.08	0.58	0.04	—	7.82	0.18	22.00	1.20	0.80
A(13)	0.65	0.35	1.95	0.05	—	—	0.22	0.04	3.40	1.08	0.06	0.14	0.02	0.04	7.93	0.07	22.00	1.70	0.30

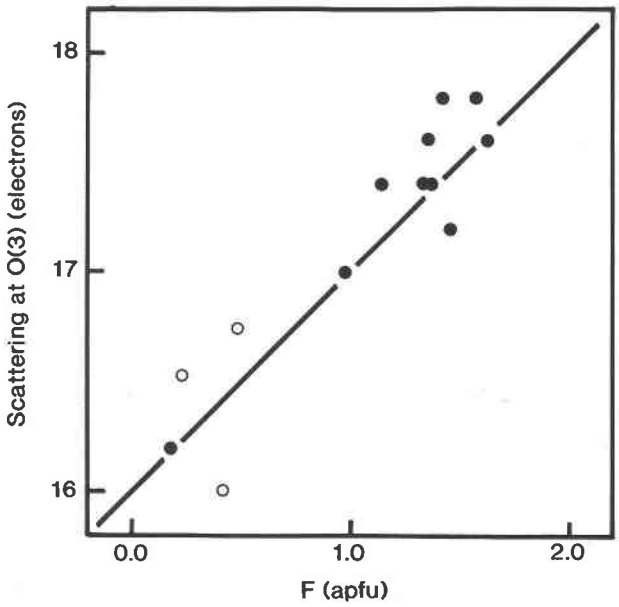

Fig. 5. Comparison of the site scattering at O3 from crystal structure refinements with the F content from the microprobe analyses. The line shows the 1:1 relationship; the open circles show data for leakeite crystals (Hawthorne et al., 1992).

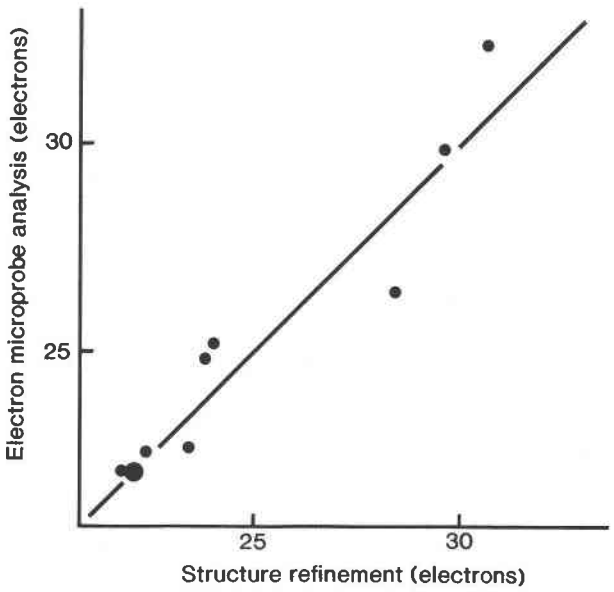

Fig. 6. Comparison of the refined scattering at M4 (expressed in terms of the number of electrons at the site) and the analogous value calculated from the B-group cations assigned from the microprobe analyses; the larger circle indicates two overlapping values.

and large, there is good agreement between the two sets of values, the data scattering about the 1:1 line. This indicates that there is no systematic difference between the results. Two crystals, A(2) and A(6), show significant differences between the two techniques; however, the differences are not systematic, and their origin is not clear. A few of the amphiboles show significant occupancy of the M4′ site (Table 5), a site occupying the same cavity as the M4 site but displaced by a small amount (~0.40 Å) toward the octahedral strip. The stereochemistry and cation occupancy of this site were examined in manganoan richterite samples by Oberti et al. (1993), who concluded that this site is occupied by $Mn^{2+} + Fe^{2+}$, in accord with the generally accepted method of cation assignment in amphiboles.

Li incorporation in the octahedral strip

The scattering and geometrical results clearly show that Li is completely ordered at the M3 site. When Li occupies M3, there is a significant decrease in the local bond valence to O1 and O3 from M3. This could be compensated by incorporation of Fe^{3+} at M1 or M2, but only the latter occurs in the amphiboles examined here. The reason for this ordering can be understood in terms of local bond-valence requirements. The anions O2 and O4 are formally underbonded in amphiboles in general and in arfvedsonite in particular (1.877 and 1.667 vu, respectively, for a Pauling, 1960, bond-strength scheme). Local bond-valence satisfaction occurs by a strong distortion of all polyhedra involving O2 (M1, M2, M4, and T2) and O4 (M2, M4, and T2). The ordering of Li at M3 is the only mechanism that avoids further underbonding of O2 and O4, and the incorporation of Fe^{3+} at M2 is the only mechanism that reduces the underbonding of O4.

In principle, there could also be a local coupling between $^{[M3]}$Li and $^{[M1]}$Ti if O3 were locally occupied by a monovalent anion. There is no relation between Li and Ti contents in these amphiboles, however, and the observed bond lengths do not indicate the presence of Ti at M1 when there is no dehydroxylation at O3. Moreover, the mechanisms of incorporation of $^{[M3]}$Li and $^{[M1]}$Ti discussed above have been separately confirmed in other less complicated amphiboles (Hawthorne et al., 1992; Oberti et al., 1992).

Compositional variations

Some of the end-member compositions and substitutions (exchange vectors) pertinent to chemical variations in arfvedsonitic amphiboles are shown in Table 9. There are two ways in which Li can enter the M1, M2, and M3 sites in ideal arfvedsonite: (1) substitution 2, whereby the charge deficiency introduced in the C-group cations is compensated by introducing a divalent cation [expressed as Ca, but (Mn,Fe,Mg) is also possible] in the B group; (2) substitution 3, whereby the charge deficiency is compensated within the C group by substituting an additional trivalent cation for a divalent cation. Inspection of Table 6 shows that although there is substantial variation in the Ca content of M4, it does not correlate significantly with Li. On the other hand, increasing Li does correlate with increasing Fe^{3+} content of the M1, M2, and M3 sites (Fig. 7b); the unit formula of crystal A(5) is particularly notable in this respect, with Li ~ 0.63 and Fe^{3+} ~ 1.86 apfu. As no other substitutions that increase the charge at the

TABLE 9. Selected end-member compositions for alkali amphiboles

	A	B	C	T		W	Name	Exchange vector
(1)	Na	Na_2	$Fe^{2+}_4Fe^{3+}$	Si_8	O_{22}	$(OH)_2$	arfvedsonite	additive component
(2)	Na	NaCa	$Fe^{2+}_5LiFe^{3+}$	Si_8	O_{22}	$(OH)_2$	—	$^{M3}LiCa(^{M3}Fe^{2+}Na)_{-1}$
(3)	Na	Na_2	$Fe^{2+}_3LiFe^{3+}_2$	Si_8	O_{22}	$(OH)_2$	—	$^{M3}LiFe^{3+}(^{M3}Fe^{2+}Fe^{2+})_{-1}$
(4)	□	Na_2	$Fe^{2+}_5Fe^{3+}_2$	Si_8	O_{22}	$(OH)_2$	riebeckite	$^{A}\square Fe^{3+}(^{A}NaFe^{2+})_{-1}$
(5)	Na	Na_2	$Fe^{2+}_3Fe^{3+}_2$	Si_7Al	O_{22}	$(OH)_2$	ferro-ferri-nyboite	$Fe^{3+}Al(Fe^{2+}Si)_{-1}$
(6)	Na	Na_2	$Fe^{2+}_2TiFe^{3+}$	Si_8	O_{22}	$(O)_2$	—	$^{M1}Ti^{H}\square_2(^{M1}Fe^{2+}{}_2{}^{H}H_2)_{-1}$

A or T sites are possible, substitution (3) must be the principal mechanism for incorporation of $^{[6]}$Li at the M1, M2, and M3 sites in these amphiboles.

Significant other substitutions are also shown in Table 9. Minor A-site vacancies (substitution 4 in Table 9), $^{[4]}$Al (substitution 5), and $^{[6]}$Ti (substitution 6) are all common features of these amphiboles but do not reach dominant proportions. Some of these chemical variations are shown in Figure 7. Increasing Li correlates strongly with increasing Fe^{3+}, and the trend shown in Figure 7a suggests significant substitution of a ferro-ferri-nyboitic component. This is examined more closely in Figure 7b; there is a significant ferro-ferri-nyboitic component, but it decreases at high $^{[6]}$Li contents. That is to be expected, as both $^{[M3]}LiFe^{3+} \rightarrow {}^{[M3]}Fe^{2+}Fe^{2+}$ and $Fe^{3+}Al \rightarrow Fe^{2+}Si$ substitutions rely on the incorporation of Fe^{3+} into the octahedral strip for charge compensation, and both trends in Figure 7 show convergence toward the ideal end-member (end-member 3 from Table 9).

Problems with alkali-amphibole analyses: Qualitative considerations

Hawthorne (1976) examined a large number of amphibole analyses of the eckermannite-arfvedsonite and magnesio-katophorite–katophorite series, and showed that when the cations are assigned to the A, B, C, and T groups in the standard way (Leake, 1968), the sums of the Y-group cations are often significantly less than the ideal minimum value of 5.0 apfu. This behavior is observed only for alkali amphiboles (and not for calcic amphiboles), indicating that this discrepancy is a real feature of alkali amphibole chemistry and not an artifact of bad analyses. Two possibilities were suggested to account for this observation: (1) small amounts of Ca occur at the M1, M2, and M3 sites; (2) Li is a significant component in these amphiboles, occurring at the M1, M2, and M3 sites.

Czamanske and Dillet (1988) reviewed the literature pertaining to the chemistry of alkali amphiboles. They noted that anomalously small C-group cation sums are common in the eckermannite-arfvedsonite amphiboles and also identified some additional problems. For example, the ratio of $Fe^{3+}/(Fe^{2+} + Fe^{3+})$ in end-member arfvedsonite is 0.20, giving an ideal Fe^{3+} content of 1.0 apfu; several studies show that $Fe^{3+}/(Fe^{2+} + Fe^{3+})$ typically exceeds 0.30 in arfvedsonite with completely occupied A sites (Fabriès and Rocci, 1972; Andersen et al., 1975; Czamanske and Dillet, 1988). Czamanske and Dillet (1988) suggested a Na-Fe^{3+} couple, analogous to

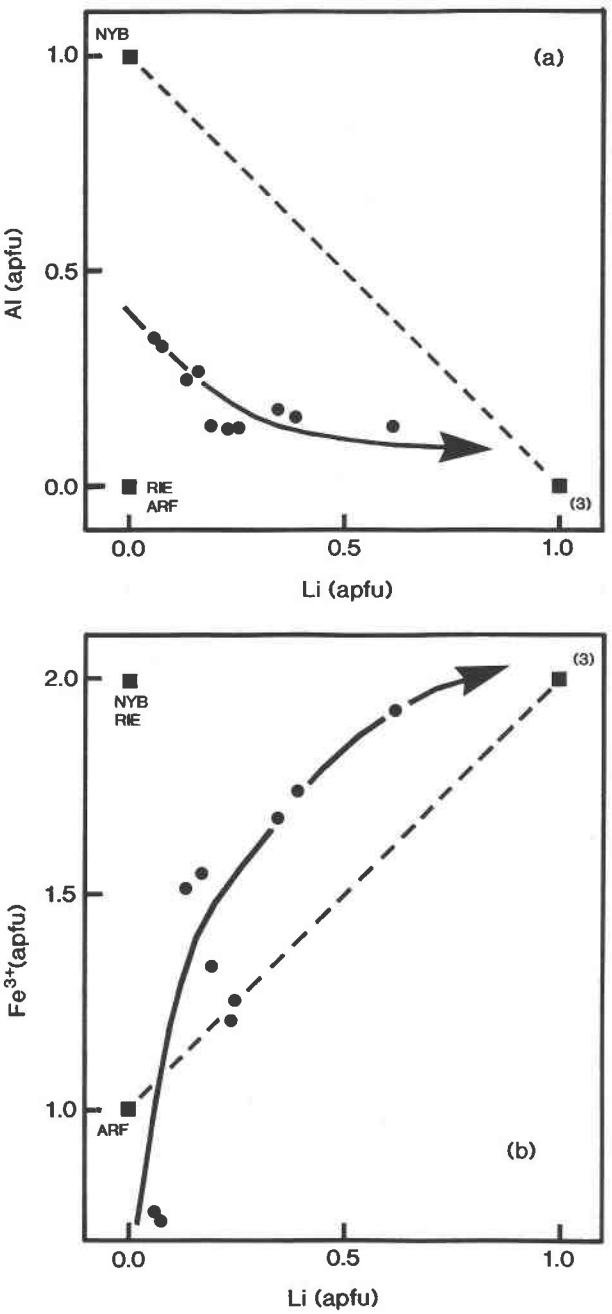

Fig. 7. (a) Variation in $^{[4]}$Al as a function of Li content; (b) variation in Fe^{3+} as a function of Li content. ARF = arfvedsonite, NYB = nyboite, RIE = riebeckite, (3) = end-member 3 from Table 9.

TABLE 10. Formula unit of amphiboles calculated on the basis of 23 O apfu, while calculating Fe^{3+}/Fe^{2+} in the usual way and omitting Li and Zn from the normalization

	A(2)	A(5)	A(6)	A(7)	A(8)	A(9)	A(10)	A(11)	A(12)	A(13)
Si	7.757	8.284	7.808	7.660	8.116	8.081	8.111	8.081	7.860	8.280
Al	0.243	0.000	0.192	0.340	0.000	0.000	0.000	0.000	0.140	0.000
Sum T	8.000	8.284	8.000	8.000	8.116	8.081	8.111	8.081	8.000	8.280
Al	0.085	0.216	0.074	0.005	0.170	0.187	0.145	0.146	0.129	0.144
Ti	0.046	0.083	0.043	0.045	0.091	0.081	0.121	0.120	0.082	0.062
Fe^{3+}	0.452	0.000	0.748	0.615	0.254	0.325	0.405	0.465	0.861	0.000
Fe^{2+}	0.958	3.243	1.481	1.228	3.453	3.381	2.626	2.451	3.168	4.352
Mg	2.976	0.488	2.099	2.562	0.151	0.212	0.671	0.783	0.297	0.005
Mn	0.483	0.619	0.555	0.544	0.766	0.733	0.923	0.954	0.463	0.155
Sum C	5.000	4.649	5.000	5.000	4.885	4.919	4.891	4.919	5.000	4.718
Ca	1.063	0.026	0.495	0.761	0.009	0.011	0.060	0.068	0.078	0.068
Na	0.973	1.974	1.505	1.239	1.991	1.989	1.940	1.932	1.922	1.932
Sum B	2.000	2.000	2.000	2.000	2.000	2.000	2.000	2.000	2.000	2.000
Na	0.396	0.923	0.576	0.694	0.881	0.868	0.718	0.730	0.670	0.487
K	0.156	0.246	0.211	0.175	0.272	0.286	0.211	0.189	0.237	0.621
Sum A	0.552	1.169	0.787	0.869	1.153	1.154	0.929	0.919	0.907	1.108

that in acmite, leading to compositions of the sort $(Na,K)Na_2(\square_{0.5}Fe^{2+}_{2.5}Fe^{3+}_2)Si_8O_{22}(OH)_2$. Hawthorne (1976) suggested that a substitution of the form $Li + Fe^{3+} \rightarrow 2Mg$ may allow incorporation of Li at the M1, M2, and M3 sites in arfvedsonite. That also causes an increase in Fe^{3+} content above the ideal value of 1.0 apfu, with the incorporation of a monovalent cation at M1, M2, and M3.

As described above, the amphiboles of this study incorporate Li at the M3 site by the substitution $^{[M3]}Li + {}^{[M2]}Fe^{3+} \rightarrow {}^{[M3]}(Fe^{2+},Mg) + {}^{[M2]}(Fe^{2+},Mg)$. This qualitatively explains two of the problems in alkali amphibole analyses identified above: not analyzing for Li will produce an apparent deficiency in the Y-group cation sums, and the substitution will also raise the Fe^{3+} content above the ideal value of 1.0 apfu in arfvedsonite with full A sites.

There are other unusual aspects of alkali amphibole analyses that are not shown by other groups of amphiboles. In particular, Si often exceeds 8.0 apfu (Stephenson and Upton, 1982; Collerson, 1982; Strong and Taylor, 1984), a result that is incompatible with the amphibole structure. It has been suggested (Ross, 1984) that such deviations from amphibole stoichiometry could be caused by fine-scale intergrowth of sodic pyroxene. However, because the compositional differences between acmite and arfvedsonite are small, such intergrowths would have to be present in significant amounts to cause the observed compositional deviations, and there should be visible diffraction effects (streaking, reflection broadening) that we have not observed in these amphiboles. That Si apparently exceeds 8.0 atoms in the unit formulae of some alkali amphiboles does seem well established. This may reflect either problems with the normalization procedure used to calculate the formula unit or problems with the chemical analyses. Which of these is actually the case will now be resolved.

Problems with alkali amphibole analyses: Quantitative considerations

The questions and problems outlined in the previous section can be considered quantitatively by comparing the unit formulae calculated as outlined previously with analogous values calculated in the standard fashion. The salient aspects of the calculations are (1) calculation based on (23 + Ti) O atoms (when Ti occurs at M1 and allowing for analyzed F) with Li determined by ion microprobe analysis, and Fe^{3+}/Fe^{2+} derived from the refined crystal structure; (2) calculation based on 23 O atoms, ignoring Li and Zn, and calculating Fe^{3+}/Fe^{2+} by means of the usual stoichiometric constraints. Values derived by method 1 are given in Table 6, and values derived by method 2 are given in Table 10.

Si content. The Si contents in Table 10 frequently exceed 8.0 apfu, reaching a maximum of 8.28 apfu and spanning the range typically shown by data from the literature. Comparison with Table 6 shows that this excess is not a feature of our best estimates of the unit formulae using complete chemical and X-ray data.

C-group sums. The C-group cation sums in Table 10 are generally lower than those of Table 6, frequently falling significantly below the ideal value of 5.0 apfu. Although the analogous sums in Table 6 are often still not ideal in this regard, the deficiencies are much less than those in Table 10 and presumably reflect the difficulty in accurately accounting for Li, H_2O, and Fe^{3+}/Fe^{2+}. In addition, the structure refinements indicate that in crystals A(7), A(10), and A(11), there is significant B-group (Mn,Fe,Mg), and the unit formulae of Table 6 are in agreement with that, whereas the unit formulae of Table 10 show significant C-group deficiencies and hence no indication of (Mn,Fe,Mg) assigned to the B group.

A-group sums. The A-group cation sums of Table 10 often significantly exceed the maximum ideal value of 1.0 apfu. This is not the case for the analogous sums in Table 6; although some do exceed 1.0 apfu, the amounts are quite small and presumably relate to normal random error in the analytical data, together with minor problems in the estimation of Li, H_2O, and Fe^{3+}/Fe^{2+}.

Fe^{3+}/Fe^{2+} ratios. The Fe^{3+}/Fe^{2+} ratios in Table 10 bear no resemblance to the analogous values in Table 6, again demonstrating the inaccuracy of this calculation procedure for amphiboles in general (cf. Fig. 7 of Hawthorne, 1983a). In principle, the calculation should work; in prac-

tice, omission of significant components (e.g., Li, Zn) and inaccurate estimation of others (e.g., H_2O) perturb both the charge and stoichiometry constraints of the calculation, to the extent that there is little correlation between the calculated Fe^{3+}/Fe^{2+} ratio and the true value. If we can better estimate these factors (e.g., Li and H contents by ion microprobe analysis), the accuracy of such calculations could be improved.

It is notable that the values of $Fe^{3+}/(Fe^{2+} + Fe^{3+})$ in Table 6 usually exceed the ideal value of 0.20 for end-member arfvedsonite. That is also the case for the 31 superior arfvedsonite analyses considered by Czamanske and Dillet (1988). Comparison of the unit formulae in Tables 6 and 10 shows that even when the amphibole has $Fe^{3+}/(Fe^{2+} + Fe^{3+}) > 0.2$ (Table 6), omission of Li and Zn and normalization of the analysis by method 2 shifts the $Fe^{3+}/Fe^{2+} + Fe^{3+})$ values to below 0.2, concealing the high oxidation ratios.

From the discussion given above, it is apparent that the problems previously encountered with the stoichiometry of arfvedsonitic amphiboles stem from (1) omission of significant components (specifically Li) from the analytical procedure, (2) inappropriate stoichiometric assumptions (particularly OH + F = 2 apfu), and (3) inappropriate renormalization procedures, resulting in incorrect $Fe^{3+}/(Fe^{2+} + Fe^{3+})$ ratios. It is obvious that the analytical problems are nontrivial, but they can be overcome by the use of combined crystal-structure refinement and electron and ion microprobe analysis.

Magmatic-subsolidus and oxidizing trends

Strong and Taylor (1984) identified two distinct trends in alkali-amphibole compositions from silica-saturated peralkaline igneous rocks. The details of these trends are shown in Figure 8. The magmatic-subsolidus trend involves a continuous change from magmatic to subsolidus amphibole, from barroisite (BAR) to richterite (RIC) to arfvedsonite (ARF). This involves the primary substitution $SiNa \rightarrow {}^{[4]}AlCa[SiNa(AlCa)_{-1}]$, which is proposed to occur under reducing conditions and involves amphiboles with full A sites. The oxidation trend involves a continuous change toward riebeckite (RIE) under the influence of oxidizing hydrothermal fluids. This involves the substitutions $Fe^{3+}Al \rightarrow Fe^{2+}Si[Fe^{3+}Al(Fe^{2+}Si)_{-1}]$ or ${}^{A}\square Fe^{3+} \rightarrow {}^{A}NaFe^{2+}[\square Fe^{3+}(NaFe^{2+})_{-1}]$, with changes toward amphiboles with vacant A sites. Thus the ideal ends of the trends involve $Fe^{3+}/(Fe^{2+} + Fe^{3+})$ values of 0.20 and 0.40, respectively.

Now let us consider the results of the current work. It is shown here that the substitution $LiFe^{3+} \rightarrow 2Fe^{2+}[LiFe^{3+}(Fe^{2+})_{-2}]$ is an important factor in the chemical variations shown by some igneous alkali amphiboles. This is a strongly oxidizing substitution, ending at the composition $NaNa_2Fe^{2+}_2Fe^{3+}_2LiSi_8O_{22}(OH,F)_2$, with a ratio of $Fe^{3+}/(Fe^{2+} + Fe^{3+})$ of 0.5. This is much more oxidizing than riebeckite, with an ideal $Fe^{3+}/(Fe^{2+} + Fe^{3+})$ ratio of 0.40; however, when the Li-bearing end-member amphibole composition (end-member 3 from Table 9) is plotted on Figure 8, it falls exactly at the position for

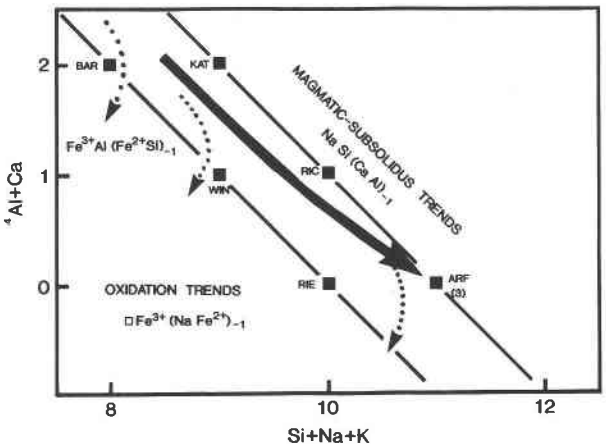

Fig. 8. Magmatic-subsolidus and oxidation trends in alkali amphiboles from silica-saturated peralkaline granites as defined by Strong and Taylor (1984); BAR = barroisite, WIN = winchite, RIE = riebeckite, KAT = katophorite, RIC = richterite, ARF = arfvedsonite. Note the coincidence of arfvedsonite [$Fe^{3+}/(Fe^{2+} + Fe^{3+}) = 0.20$] with end-member 3 of Table 9, with $Fe^{3+}/(Fe^{2+} + Fe^{3+}) = 0.50$.

arfvedsonite [with an $Fe^{3+}/(Fe^{2+} + Fe^{3+})$ ratio of 0.20]. Thus it is apparent that the trend labeled magmatic-subsolidus in Figure 8 can be far more oxidizing than the trend labeled oxidation if the $LiFe^{3+} \rightarrow {}^{2}Fe^{2+}$ substitution is involved. Indeed, this result explains the stability of these arfvedsonitic amphiboles in the Questa rocks, which are characterized by the relatively oxidized assemblage titanite + magnetite + quartz (Wones, 1989).

On the basis of the data and arguments presented here, it is apparent that Strong and Taylor's (1984) proposal of two distinct trends in alkali amphibole composition is formulated in a misleading manner. Among others, the work of Czamanske and Wones (1973), Czamanske et al. (1977, 1981), and Czamanske and Dillet (1988) showed that, during magmatic crystallization, trends in amphibole (and biotite) compositions may record either progressive oxidation or reduction. However, the basic premise of Strong and Taylor (1984) is that the compositional trend for magmatic-subsolidus conditions involves substitutions under reducing conditions. At Questa, both the titanite + magnetite + quartz assemblage and the amphibole formulae show that magmatic conditions were oxidizing, and yet they produced arfvedsonite amphiboles. This does not invalidate the general idea of magmatic-subsolidus and hydrothermal compositional trends in such alkali amphiboles. Indeed, it is well established that the latter involves the formation of A-site vacant amphiboles (riebeckite), without implying oxidation relative to the f_{O_2} extant during crystallization of primary amphiboles (Mitchell, 1990). However, the results given here do invalidate the idea of compositional trends developed under magmatic-subsolidus conditions being universally reducing.

It is apparent that the degree of oxidation should be analyzed directly rather than inferred indirectly from incomplete analyses, particularly when such influences as

the $LiFe^{3+} \rightarrow 2Fe^{2+}$ substitution may be important. Alkali amphiboles need complete analyses (i.e., including Li, Zn, and F), and analytically derived Fe^{3+}/Fe^{2+} ratios are of critical importance in understanding their paragenetic behavior.

Conclusions

1. Li can be a significant component in alkali amphiboles from igneous environments. In arfvedsonitic amphiboles, Li reaches at least 0.60 apfu (~1.0 wt% Li_2O).

2. Li is completely ordered at the M3 site in these alkali amphiboles.

3. Mn and Zn can be significant components in alkali amphiboles, reaching at least 0.92 and 0.10 apfu (6.9 and 0.9 wt%), respectively.

4. Mean bond lengths and charge-balance considerations show Fe^{3+} to be present in amounts considerably exceeding the ideal value of 1.0 apfu for end-member arfvedsonite.

5. Significant B-group occupancy by (Mn,Fe) can be detected by crystal structure refinement by means of occupancy of the M4′ site, a position very similar to the M4 site in monoclinic ferromagnesian amphiboles.

6. The scattering at the M1, M2, and M3 sites, the M4 and M4′ sites, and the O3 site all agree closely with the effective scattering (number of electrons) calculated from unit formulae derived from electron and ion microprobe analyses. This suggests that the rather complicated procedure used here to derive the unit formulae is reasonably accurate.

7. The $^{[6]}Li$ can be a major C-group cation in alkali amphiboles; it enters into the structure by means of the substitution $Li + Fe^{3+} \rightarrow 2Fe^{2+}[LiFe^{3+}(Fe^{2+})_{-2}]$.

8. Stoichiometry problems previously encountered in arfvedsonitic amphiboles were largely due to the omission of Li and Zn from the analysis and to inappropriate renormalization procedures.

9. Previous graphical representations of magmatic-subsolidus and oxidation trends in alkali amphiboles from silica-saturated peralkaline igneous rocks do not take into consideration the $Li + Fe^{3+} \rightarrow 2Fe^{2+}$ substitution. When this substitution is significant, the usual graphical methods of representing these trends can give totally misleading results. We recommend that $Fe^{3+}/(Fe^{2+} + Fe^{3+})$ ratios be used directly for this purpose.

Acknowledgments

We thank M. Palenzona for his help in preparing samples and for technical assistance with the ion microprobe analyses and Alison Pawley and Ric Wendlandt for their reviews of the manuscript. Financial support for this work was provided by the Natural Sciences and Engineering Research Council of Canada and CNR-NATO.

References cited

Andersen, E.B., Fenger, J., and Rose-Hansen, J. (1975) Determination of $[Fe^{2+}]/[Fe^{3+}]$-ratios in arfvedsonite by Mössbauer spectroscopy. Lithos, 8, 237–246.

Borley, G.D. (1963) Amphiboles from the younger granites of Nigeria. I. Chemical classification. Mineralogical Magazine, 33, 358–376.

Collerson, K.D. (1982) Geochemistry and Rb-Sr geochronology of associated proterozoic peralkaline anorogenic granites from Labrador. Contributions to Mineralogy and Petrology, 81, 126–147.

Czamanske, G.K., and Dillet, B. (1988) Alkali amphibole, tetrasilicic mica, and sodic pyroxene in peralkaline siliceous rocks, Questa Caldera, New Mexico. American Journal of Science, 288A, 358–392.

Czamanske, G.K., and Wones, D.R. (1973) Oxidation during magmatic differentiation, Finnmarka complex, Oslo area, Norway. II. The mafic silicates. Journal of Petrology, 14, 349–380.

Czamanske, G.K., Wones, D.R., and Eichelberger, J.C. (1977) Mineralogy and petrology of the intrusive complex of the Pliny Range, New Hampshire. American Journal of Science, 277, 1073–1123.

Czamanske, G.K., Ishihara, S., and Atkin, S.A. (1981) Chemistry of rock-forming minerals of the Cretaceous-Paleocene batholith in Southwestern Japan and implications for magma genesis. Journal of Geophysical Research, 86, 10431–10469.

de Keyser, F. (1966) Arfvedsonite in granites of the Ingham district, North Queensland. Contributions to Mineralogy and Petrology, 12, 315–324.

Fabriès, J., and Rocci, G. (1972) Evolution cristallochimique des amphiboles dans la série de Fort-Trinquet (Mauritanie). Contributions to Mineralogy and Petrology, 35, 215–225.

Ghose, S., Kersten, M., Langer, K., Rossi, G., and Ungaretti, L. (1986) Crystal field spectra and Jahn-Teller effect of Mn^{3+} in clinopyroxenes and clinoamphiboles from India. Physics and Chemistry of Minerals, 13, 291–305.

Giret, A., Bonin, B., and Leger, J.-M. (1980) Amphibole compositional trends in oversaturated and undersaturated alkaline plutonic ring-complexes. Canadian Mineralogist, 18, 481–495.

Hawthorne, F.C. (1976) The crystal chemistry of the amphiboles. V. The structure and chemistry of arfvedsonite. Canadian Mineralogist, 14, 346–356.

——— (1978) The crystal chemistry of the amphiboles. VIII. The crystal structure and site chemistry of fluor-riebeckite. Canadian Mineralogist, 16, 187–194.

——— (1983a) The crystal chemistry of the amphiboles. Canadian Mineralogist, 21, 173–480.

——— (1983b) Quantitative characterization of site occupancies in minerals. American Mineralogist, 68, 287–306.

Hawthorne, F.C., and Grundy, H.D. (1977) The crystal chemistry of the amphiboles. III. Refinement of the crystal structure of a subsilicic hastingsite. Mineralogical Magazine, 41, 43–50.

Hawthorne, F.C., Oberti, R., Ungaretti, L., and Grice, J.D. (1992) Leakeite, $NaNa_2(Mg_2Fe^{3+}_2Li)Si_8O_{22}(OH)_2$, a new alkali amphibole from the Kajlidongri manganese mine, Jhabua district, Madhya Pradesh, India. American Mineralogist, 77, 1112–1115.

Johnson, C.M., Czamanske, G.K., and Lipman, P.W. (1989) Geochemistry of intrusive rocks associated with their Latir volcanic field, New Mexico, and contrasts between evolution of plutonic and volcanic rocks. Contributions to Mineralogy and Petrology, 103, 90–109.

Johnson, C.M., Lipman, P.W., and Czamanske, G.K. (1990) H, O, Sr, Nd, and Pb isotope geochemistry of the Latir volcanic field and cogenetic intrusions, New Mexico, and relations between evolution of a continental magmatic center and modifications of the lithosphere. Contributions to Mineralogy and Petrology, 104, 99–124.

Kawahara, A. (1963) X-ray studies on some alkaline amphiboles. Mineralogical Journal (Japan), 4, 30–40.

Kitamura, M., Tokonami, M., and Morimoto, N. (1975) Distribution of titanium atoms in oxy-kaersutite. Contributions to Mineralogy and Petrology, 51, 167–172.

Leake, B.E. (1968) A catalog of analyzed calciferous and subcalciferous amphiboles together with their nomenclature and associated minerals. Geological Society of America Special Paper, 98, 1–210.

Mitchell, R.H. (1990) A review of the compositional variation of amphiboles in alkaline plutonic complexes. Lithos, 26, 135–156.

Neumann, E.-R. (1976) Compositional relations among pyroxenes, amphiboles and other mafic phases in the Oslo region plutonic rocks. Lithos, 9, 85–109.

Oberti, R., Ungaretti, L., Cannillo, E., and Hawthorne, F.C. (1992) The behaviour of Ti in amphiboles. I. Four- and six-coordinate Ti in richterite. European Journal of Mineralogy, 4, 425–439.

Oberti, R., Hawthorne, F.C., Ungaretti, L., and Cannillo, E. (1993) The

behaviour of Mn in amphiboles: Mn in richterite. European Journal of Mineralogy, 5, 43–52.

Ottolini, L., Bottazzi, P., Vanucci, R. (1992) SIMS investigation of Li, Be, B in silicate minerals using CEF. Goldschmidt Conference Abstracts, A-81.

Pauling, L. (1960) The nature of the chemical bond (3rd edition), 644 p. Cornell University Press, Ithaca, New York.

Ross, M. (1984) Ultraalkalic arfvedsonite and associated richterite, acmite, and aegerine-augite in quartz syenite, Magnet Cove alkalic igneous complex, Arkansas. Eos, 65, 293.

Stephenson, D., and Upton, B.G.J. (1982) Ferromagnesian silicates in a differentiated alkaline complex: Kungnat Fjeld, South Greenland. Mineralogical Magazine, 46, 283–300.

Strong, D.F., and Taylor, R.P. (1984) Magmatic-subsolidus and oxidation trends in composition of amphiboles from silica-saturated peralkaline igneous rocks. Tschermaks mineralogisch-petrologische Mitteilungen, 32, 211–222.

Ungaretti, L., Mazzi, F., Rossi, G., and Dal Negro, A. (1978) Crystal-chemical characterization of blue amphiboles. Proceedings of the XI General Meeting of the IMA, Rock-Forming Minerals, 82–110.

Ungaretti, L., Lombardo, B., Domeneghetti, C., and Rossi, G. (1983) Crystal-chemical evolution of amphiboles from eclogitized rocks of the Sesia Lanzo Zone, Italian western Alps. Bulletin de Minéralogie, 106, 645–672.

Wones, D.R. (1989) Significance of the assemblage titanite + magnetite + quartz in granitic rocks. American Mineralogist, 74, 744–749.

Manuscript received June 5, 1992
Manuscript accepted March 5, 1993

AM-93-529

Li: An important component in igneous alkali amphiboles

Frank C. Hawthorne, Luciano Ungaretti, Roberta Oberti, Piero Bottazzi, Gerald K. Czamanske

For deposit: Table 3

American Mineralogist, 78, 7-8, 733-745.

Table 3. Atomic coordinates (x 10^4) and equivalent isotropic displacement parameters ($Å^2$).

No.	O(1)				O(2)				O(3)				O(4)				O(5)			
	x/a	*y/b*	*z/c*	B_{eq}	*x/a*	*y/b*	*z/c*	B_{eq}	*x/a*	*y/b*	*z/c*	B_{eq}	*x/a*	*y/b*	*z/c*	B_{eq}	*x/a*	*y/b*	*z/c*	B_{eq}
A(1)	1125	860	2185	0.58	1183	1684	7257	0.70	1028	0	7121	0.89	3625	2494	7950	0.93	3492	1334	947	0.93
A(2)	1123	866	2183	0.72	1186	1686	7272	0.68	1034	0	7103	0.89	3623	2494	7961	0.86	3490	1327	945	0.97
A(3)	1107	906	2088	0.65	1198	1715	7368	0.64	1130	0	7071	1.12	3652	2497	8013	0.81	3507	1284	836	0.82
A(4)	1107	904	2093	0.61	1197	1714	7363	0.61	1123	0	7067	1.03	3651	2498	8012	0.78	3505	1284	834	0.77
A(5)	1108	907	2088	0.59	1200	1718	7373	0.62	1130	0	7075	1.08	3654	2496	8011	0.78	3506	1284	831	0.79
A(6)	1119	871	2147	0.71	1199	1699	7291	0.82	1072	0	7098	0.92	3634	2485	7952	1.02	3482	1302	874	0.95
A(7)	1120	863	2155	0.72	1198	1697	7277	0.76	1061	0	7112	0.92	3629	2485	7936	1.01	3480	1308	887	0.98
A(8)	1113	905	2073	0.67	1201	1720	7365	0.70	1116	0	7081	1.00	3653	2490	8000	0.91	3498	1282	811	0.89
A(9)	1111	909	2071	0.67	1202	1721	7376	0.70	1119	0	7082	1.12	3656	2490	8001	0.86	3496	1283	814	0.85
A(10)	1127	881	2102	0.75	1206	1707	7320	0.81	1097	0	7088	1.11	3640	2484	7965	1.11	3491	1278	798	0.94
A(11)	1126	884	2097	0.71	1207	1709	7324	0.76	1099	0	7083	1.07	3643	2484	7970	1.05	3491	1278	795	0.88
A(12)	1111	903	2079	0.72	1202	1720	7349	0.71	1112	0	7076	1.00	3649	2488	7986	0.94	3488	1283	798	0.93
A(13)	1101	913	2077	0.78	1202	1726	7332	0.84	1082	0	7081	0.99	3640	2475	7992	1.02	3449	1268	804	0.86

No.	O(6)				O(7)				T(1)				T(2)				M(1)			
	x/a	*y/b*	*z/c*	B_{eq}	*x/a*	*y/b*	*z/c*	B_{eq}	*x/a*	*y/b*	*z/c*	B_{eq}	*x/a*	*y/b*	*z/c*	B_{eq}	*x/a*	*y/b*	*z/c*	B_{eq}
A(1)	3460	1198	5886	0.81	3414	0	2956	0.97	2834	845	2973	0.47	2896	1708	8041	0.46	0	839	5000	0.82
A(2)	3455	1194	5897	0.80	3404	0	2962	1.05	2826	846	2976	0.48	2895	1706	8045	0.48	0	846	5000	0.72
A(3)	3417	1201	5805	0.81	3356	0	2992	0.87	2797	858	2918	0.46	2903	1707	8024	0.45	0	888	5000	0.63
A(4)	3420	1202	5806	0.75	3358	0	2987	0.84	2797	858	2920	0.42	2902	1707	8025	0.41	0	888	5000	0.59
A(5)	3416	1202	5804	0.74	3352	0	2987	0.85	2796	859	2916	0.44	2904	1708	8026	0.42	0	889	5000	0.61
A(6)	3430	1186	5852	0.92	3385	0	2936	1.03	2805	849	2937	0.49	2891	1704	8013	0.51	0	892	5000	0.64
A(7)	3435	1181	5864	0.92	3397	0	2922	0.96	2809	847	2945	0.47	2890	1705	8014	0.49	0	892	5000	0.59
A(8)	3407	1203	5783	0.88	3340	0	2979	0.94	2801	857	2906	0.48	2903	1704	8012	0.47	0	906	5000	0.61
A(9)	3404	1203	5781	0.86	3332	0	2985	0.94	2801	858	2908	0.47	2903	1704	8018	0.46	0	906	5000	0.63
A(10)	3421	1188	5782	0.96	3376	0	2937	0.98	2806	851	2902	0.49	2898	1700	7988	0.48	0	906	5000	0.59
A(11)	3419	1189	5780	0.90	3375	0	2940	1.00	2805	851	2901	0.46	2898	1700	7989	0.46	0	908	5000	0.58
A(12)	3405	1200	5781	0.91	3341	0	2970	1.00	2801	857	2902	0.46	2899	1705	8002	0.49	0	908	5000	0.60
A(13)	3376	1183	5814	0.92	3276	0	2972	1.03	2750	860	2909	0.55	2867	1708	7998	0.55	0	909	5000	0.73

Table 3. (cont.)

No.	M(2)				M(3)				M(4)				M(42)				A			
	x/a	*y/b*	*z/c*	B_{eq}	*x/a*	*y/b*	*z/c*	B_{eq}	*x/a*	*y/b*	*z/c*	B_{eq}	*x/a*	*y/b*	*z/c*	B_{eq}	*x/a*	*y/b*	*z/c*	B_{eq}
A(1)	0	1792	0	0.61	0	0	0	0.50	0	2767	5000	1.03	-	-	-	-	0	5000	0	6.98
A(2)	0	1795	0	0.61	0	0	0	0.58	0	2774	5000	0.87	-	-	-	-	0	5000	0	5.90
A(3)	0	1811	0	0.53	0	0	0	0.67	0	2776	5000	1.11	-	-	-	-	0	5000	0	4.86
A(4)	0	1810	0	0.48	0	0	0	0.66	0	2775	5000	1.17	-	-	-	-	0	5000	0	4.69
A(5)	0	1811	0	0.50	0	0	0	0.64	0	2776	5000	1.13	-	-	-	-	0	5000	0	5.58
A(6)	0	1808	0	0.59	0	0	0	0.76	0	2761	5000	1.33	-	-	-	-	0	5000	0	7.67
A(7)	0	1804	0	0.59	0	0	0	0.56	0	2762	5000	1.20	0	2517	5000	0.63	0	5000	0	7.84
A(8)	0	1826	0	0.55	0	0	0	0.62	0	2776	5000	1.24	-	-	-	-	0	5000	0	6.30
A(9)	0	1827	0	0.56	0	0	0	0.63	0	2780	5000	1.20	-	-	-	-	0	5000	0	8.03
A(10)	0	1823	0	0.57	0	0	0	0.62	0	2761	5000	1.29	0	2577	5000	0.42	0	5000	0	4.44
A(11)	0	1824	0	0.55	0	0	0	0.63	0	2761	5000	1.35	0	2567	5000	0.68	0	5000	0	4.39
A(12)	0	1829	0	0.57	0	0	0	0.59	0	2770	5000	1.42	-	-	-	-	0	5000	0	9.90
A(13)	0	1839	0	0.59	0	0	0	0.68	0	2778	5000	1.36	-	-	-	-	0	5000	0	3.19

No.	A(m)				A(2)				H			
	x/a	*y/b*	*z/c*	B_{eq}	*x/a*	*y/b*	*z/c*	B_{eq}	*x/a*	*y/b*	*z/c*	B_{eq}
A(1)	469	5000	1117	3.60	0	4833	0	3.96	-	-	-	-
A(2)	451	5000	1077	3.84	0	4795	0	3.07	-	-	-	-
A(3)	456	5000	973	3.52	0	4693	0	3.69	-	-	-	-
A(4)	447	5000	963	3.25	0	4661	0	2.06	-	-	-	-
A(5)	449	5000	989	3.54	0	4734	0	2.17	-	-	-	-
A(6)	429	5000	958	3.41	0	4794	0	4.73	-	-	-	-
A(7)	396	5000	948	3.63	0	4802	0	3.97	-	-	-	-
A(8)	480	5000	1055	2.96	0	4617	0	2.94	1965	0	7329	4.79
A(9)	443	5000	1041	3.22	0	4498	0	1.33	2020	0	7780	1.33
A(10)	445	5000	965	3.53	0	4675	0	4.78	-	-	-	-
A(11)	440	5000	981	3.34	0	4694	0	2.49	-	-	-	-
A(12)	476	5000	1147	2.48	0	4621	0	4.44	1983	0	7472	1.61
A(13)	386	5000	937	3.24	0	4700	0	3.00	1870	0	7480	0.82